EFFECT OF PARTICLE SIZE ON PROPERTIES OF AlSi10Mg ALLOY PRODUCED BY LASER POWDER BED FUSION

POPESCU George
Facultatea: I.I.R., Specializarea: I.N.P.N., email: popescu.gh.george@gmail.com

Scientific coordinators: Prof. Dr. Ing. **Daniel GHICULESCU**
Prof. Dr. Ing. **Riccardo CASATI**

RESUME: The term of „additive manufacturing" refers to the technology that grow three-dimensional objects, one superfine layer at a time. Each successive layer bonds to the preceding layer of material. Different materials can be used, ranging from metal powder, ceramics, composites, to glass or even edibles materials. Objects are digitalized into CAD models that are used to create the .stl files. These will be sliced into thin layers and used by the machine to define the printing process. Going from .stl file to 3D is a revolutionizing manufacturing. Without the need of intermediary steps like creation of molds or dies, there is also a decrease in the production cost. Several AM techniques have been developed during recent year, two main categories being Direct Metal Deposition (DMD) and Powder Bed Fusion (PBF). This paper is focused on the Powder Bed Fusion category, more specific on the Selective Laser Melting process. The aim is to optimize the printing parameters for AlSi10Mg by printing simple geometry samples with different process parameters and evaluate the relative density of the specimens.

KEY WORDS: Additive Manufacturing (AM), AlSi10Mg, Selective Laser Melting (SLM)

1. Introduction

Additive manufacturing, also known as 3D printing, has been considered an environmentally friendly manufacturing technology which brings great benefits, such as production efficiency, material saving and less energy consumption. The process is based on successive material deposition at designated areas by delivering energy to it, transforming how products are designed and produced. This exclusive feature allows production of complex or customized parts directly from the design without the need for tools [2]. Still, knowledge about suitable materials is limited, especially in the Selective Laser Melting field (SLM).

The aim of this study is to characterize AlSi10Mg alloy parts made using AM technology. Upon printing, the solidification features and morphology, microstructure development, area of porosity and crystallographic texture orientation are elaborated. Using the optimization parameters technique, simple geometry samples like cubes were printed maintaining the power constant and varying the scanning speed in each cube with a different layer thickness and hatch spacing. Thus, each cube was manufactured with different volumetric energy density (VED).

$$VED = \frac{P}{vht}\left[\frac{J}{mm^3}\right] \quad (1)$$

P = Laser power v = Scan speed h = hatch distance t = Layer thickness

The basic principle of how Additive Manufacturing works is presented in the following workflow:

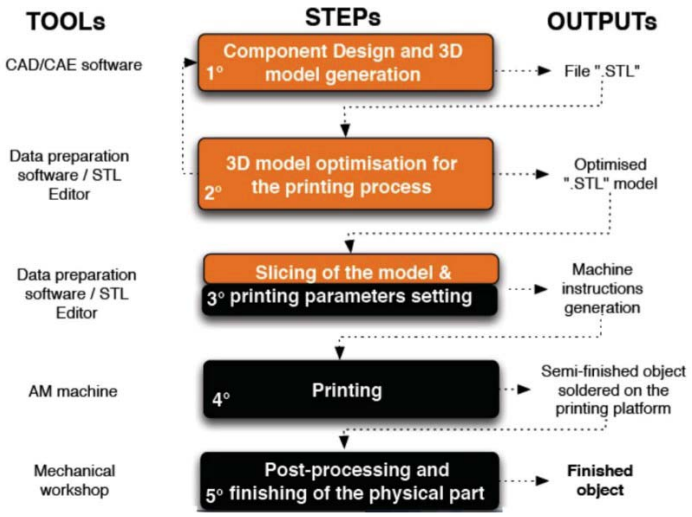

Fig. 1.Workflow for the design and manufacturing of AM parts [3]

2. Current stage

Additive manufacturing uses data CAD software or 3D object scanners to direct hardware to deposit material, layer upon layer, in precise geometric shapes. As its name implies, material is added to create an object (Fig.2). By contrast, when you create an object by traditional means, it is necessary to remove material through milling, machining, carving, shaping or other means (Fig.3).

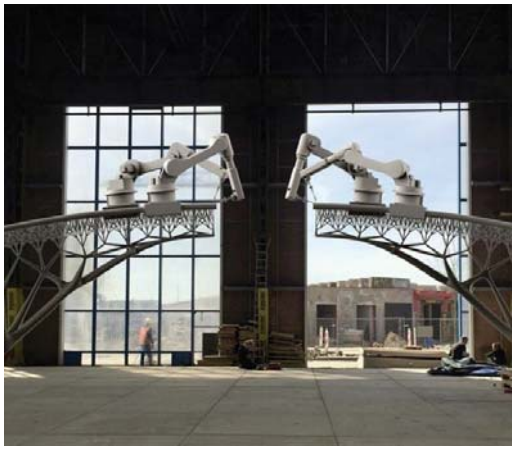

Fig. 2.Bridge construction with Direct Metal Deposition

Fig. 3.Milling process

AM is now widely accepted as a new manufacturing technique for the production of high-performance components for automotive, aerospace and medical applications [1]. Additive manufacturing may seem new to many, but it has been around for several decades. In the right applications, it delivers improved performance, complex geometries and simplified fabrication.

While traditional manufacturing is suited for mass production, 3D printing has a lower cost production when it comes to higher part complexity. This feature leads to the use of AM only when the component complexity is high or the number of parts to produce is low. From the future perspective, 3D printing will be optimized enough to be used for large scale production.

In the current stage of the research, AlSi10Mg samples were manufactured and one half of each „cube" was subjected to metallographic cleaning for microstructural characterization, while the other half is meant for heat treatment.

3. Powder Bed Fusion

Out of the AM techniques, the current study is focused on a Powder Bed Fusion process, which is designed to create parts using a high-power density laser in order to melt and fuse metallic powders together, layer by layer. It is the most widely used metal additive manufacturing process, able to produce complex parts that can't be produced by conventional manufacturing means. Beside being so popular, it has it's challenges which include high material costs, slow process speed, laborious post-processing requirements and restrictions on material compatibility. Powder bed technology is separated into three techniques: SLM, EBM and Binderjet, out of which the current research is focused on the first.

4. Selective Laser Melting

Selective laser melting is and additive manufacturing technique that allows the production of metallic parts with high mechanical properties and complex geometries, usually difficult or impossible to manufacture using conventional methods. Advantages offered by the SLM technique go from the reduction of the product mass, consequently minimizing the wasted material to the reduction of the production time of the manufacturing process where the amount requested is little and the design continuously changes, such as: the racing world and the biomedical field.

Optimal fabrication of parts using SLM requires a comprehensive understanding of the main processing parameters. In SLM, the energy input, powder bed properties and build conditions are the leading factors that affect the part quality. This can be managed in various ways, including the final part density, mechanical properties and surface finishing [10].

The laser energy density (E_ρ) can be defined using the equation below:

$$E_\rho = \frac{P}{u\delta}\left[\frac{J}{mm^3}\right] \qquad (2)$$

P – Laser Power [W]
δ – Laser Beam Diameter [mm]
μ – Laser Scanning Speed [mm/s]

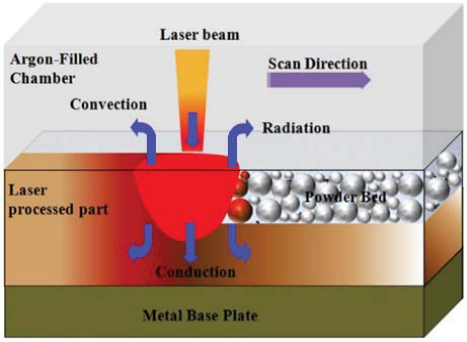

Fig. 4. Schematic representation of powder bed laser melting [3]

In the selective laser melting process, a powder layer is applied on a building platform by a recoater and a laser beam selectively scans the powder according to the CAD-data to completely melt and fuse the metal powder particles together and create fully dense materials that have mechanical properties similar to those of conventional manufactured metals. After one layer of powder is finished scanning, the platform is lowered by 20 to 100 μm and a new powder layer is applied. The operation is repeated (for a few thousands cylces, depending on the height of the part) untill the built part is finished (Fig.5)(Fig.6).

Since the SLM process is based on the component production through consolidation of different layers of metallic powder progressively overlapped between each other, a significant influence on the result is given by the powder characteristics. The powder size and morphology influence the flowability of the powder, which presents the property to uniformly spread on the building platform. Aside from powder size, the particle geometry also influence the process, causing anisotropy during the cooling.

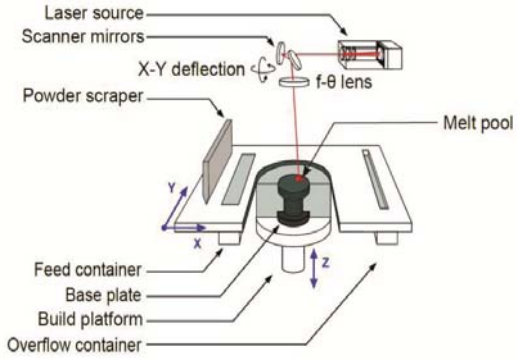

Fig. 5.Schematic overview of SLM Machine [4]

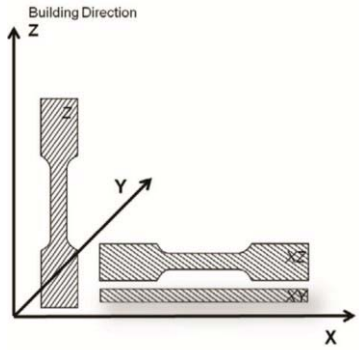

Fig. 6.Building direction of test samples [4]

For these reasons, the use of spherical powders is recommended in the Laser melting process. Powder produced via gas atomization are preferred to those made by water atomization, which are more irregular. Due to the fine particle size, it is important to maintain the unused powder in a cool, dry place, because it may retain high moisture contents which will affect the flowability and so, the distribution uniformity on the build plate. The most common powder defects are as follow:

- Irregular powder shape (Fig.8)
- Satellites: small powder grains attached to the surface of bigger grains (Fig.9)
- Hollow particles with open or closed porosity (Fig.10)

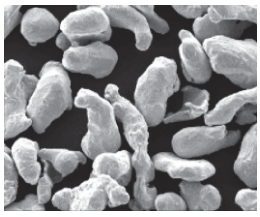

Fig. 7.Irregular powder shape [3]

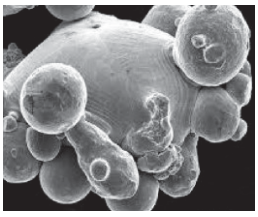

Fig. 8.Satellites attached to metal grains [3]

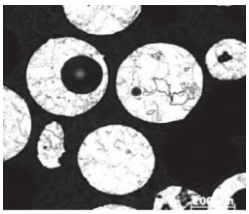

Fig. 9.Hollow particles with open porosity [3]

The main challenges of parts made by SLM are the surface roughness, part accuracy and residual stresses, which are reinforced by the thermal gradients due to full melting and solidification in a very short time. Among the defects of the process can be highlighted:

- Porosity (Fig.11) or incomplete fusion: generated by low or high VED, spatters, fumes, balling, oxide wetting, inhomogeneous powder distribution or gas pores in powder (hollow particles);
- Inhomogeneous microstructure;
- Inclusions (Fig.12): resulted from the powder used in the process, bad cleaning of the printing chamber or oxides formed during the AM process;
- Residual stresses and crack (Fig.13).

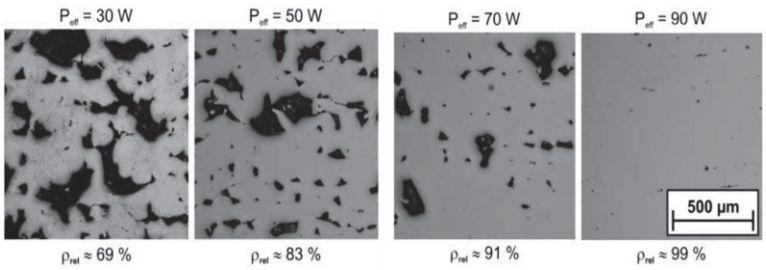

Fig. 10.Micrographs showing cross sections for different effective laser powers. The porosity decreases with increasing laser power (ρ_{rel}=relative material density) [5]

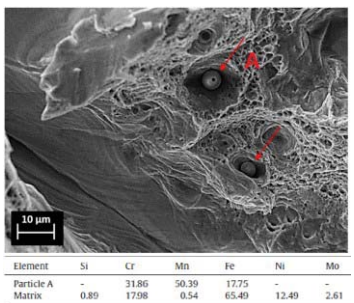

Fig. 11. MnCrFe inclusion in 316L [6]

5. Experimentation

SLM process is carried out on Renishaw AM 250 with controlled atmosphere. In this process a laser source scan powder bed according to the CAD data and manufactured 3D part. All cube samples were produced with varying hatch distance, scanning speed and point distance, keeping the other process parameters constant. In the following tables can be found the process parameters used for each specimen manufacturing. The experimentation was carried out on AlSi10Mg alloy. nalit

Table 1. AlSi10Mg 20-63 printing parameters

	Hd [mm]	Pd [µm]	V [mm/s]	Dens. En. [J/mm3]
A	0.08	60	267.9	233.3333
B	0.1	60	357.1	186.6667
C	0.12	60	446.4	155.5556
D	0.08	80	267.9	175
E	0.1	80	357.1	140
F	0.12	80	446.4	116.6667
G	0.08	100	267.9	140
H	0.1	100	357.1	112
I	0.12	100	446.4	93.33333

Table 2. AlSi10Mg 63-105 printing parameters

	Hd [mm]	Pd [µm]	V [mm/s]	Dens. En. [J/mm3]
A	0.08	60	267.9	233.3333
D	0.1	60	267.9	186.6667
G	0.12	60	267.9	155.5556
B	0.08	80	357.1	175
E	0.1	80	357.1	140
H	0.12	80	357.1	116.6667
C	0.08	100	446.4	140
F	0.1	100	446.4	112
I	0.12	100	446.4	93.33333

Using Nikon Eclipse LV150NL for SEM (scanning electron microscope), analysis is performed up to 1000X magnification. For the microscopic observation samples preparation was done as follow:
→ After printing, the specimens were cutted with a hacksaw from the base plate, separated and added into different marked plastic bags.
→ Using the abrasive cutting machine, the samples were split into two, one half following to be prepared for metallographic cleaning and microscopic observation, while the other was reserved for heat treatment.

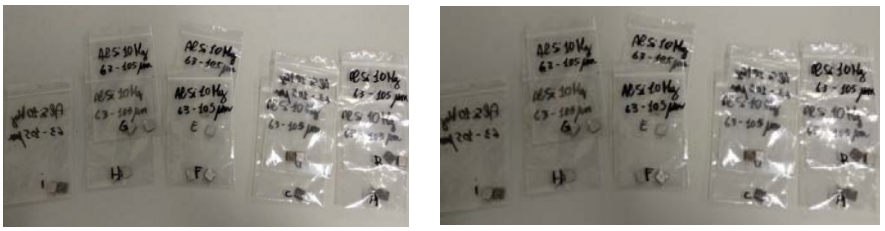

Fig. 12.Halved AlSi10Mg samples (20-63 µm and 63-105 µm)

Fig. 13.AlSi10Mg samples

→With the help of the mounting press, the samples designed for metallographic cleaning were enveloped into a polymeric resin, which made them more maneuverable. Then a signograph was used to add a differentiating mark on each enveloped specimen to keep track of them

Fig. 14.Signograph

Fig. 15.Marked Specimens

→The polishing machines, made by Hitech Europe, have been used in the Metallurgy Department from Politecnico di Milano in order to polish the samples with different abbrasive papers. The following range

of grit sizes was used to prepare the samples for the surface finishing: P120-P600-P800-P1200-P1500-P2500

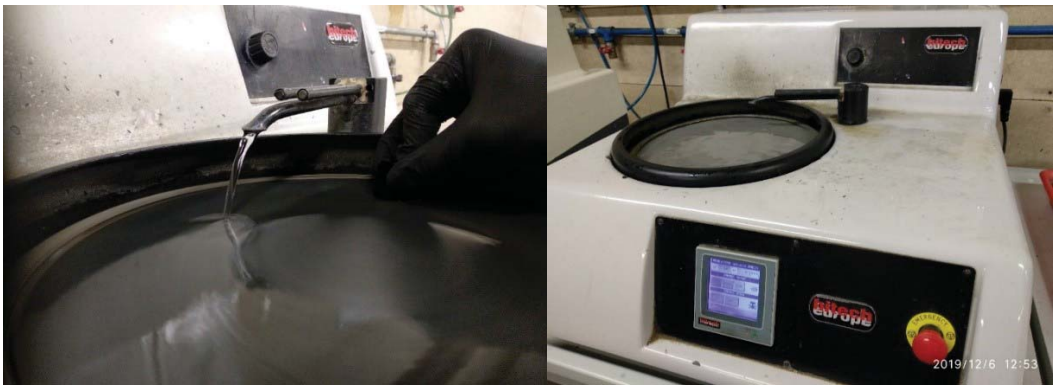

Fig. 16. Polisher Saphir 550 ATM

→The process continued with surface finishing using the MP series machines equipped with fiberglass cloth of 6µm and 1µm in order to achieve the desired results.

Fig. 17. MP22/32 Double Plate Series

Fig. 18. Polishing Lubricant

Fig. 19. Diamond suspension (particle size of 6µm and 1µm)

A tensile test was conducted on the samples, according to ASTM E8/E8M standard using a microhardness tester FM-810 Series. As per the ASTM E8/E8M regular Vickers hardness tester is used to determine hardness by measuring the resistance of the material to plastic deformation from a standard source. The payload used for the test was 100gr.

Table 3. Hardness results 20-63µm samples [HV]

Particle size 20-63 µm		
A	B	C
96.16	82.08	84.48
D	E	F
77.74	82.19	76.09
G	H	I
85.91	92.15	90.08

Table 4. Hardness results 63-105µm samples [HV]

Particle size 63-105 µm		
A	B	C
112.16	107	98.48
D	E	F
110.2	91.47	89.04
G	H	I
96.32	94.34	109.8

6. Density evaluation

With the help of Image J, a java based image analysis software, we were able to determine the optical density of the samples and create a graph for each category (20-63 µm; 63-105 µm) in order to see which parametter has a higher influence on the density of the specimens.

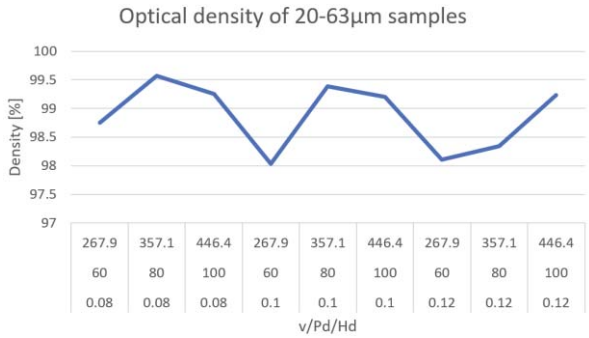

Fig. 20. Graphic representation of density variation for 20-63 µm samples

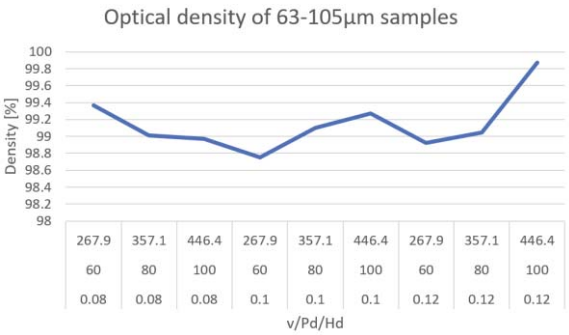

Fig. 21. Graphic representation of density variation for 63-105 µm samples

In the previous graphics (Fig.22) (Fig.23) is presented the variation of density for the investigated samples. Each parameter has 3 values which were grouped for a better understanding of the influence on the density. Hd was randomly chosen as the main parameter for the assortment. From what it can be observed, for the particle size interval of 20-63 µm samples, the density peaks correspond to a point distance of 80µm for a hatch distance of 0.08mm and 0.1mm with a scan speed of 375.1 mm/s. On the other hand, the 63-105 µm sample density peaked at the highest process parameter values. The microstructure was analyzed by observing the polished cross section using optical microscopy, considering only the horizontal orientation investigated. Chemical etching was performed, applying Keller's reagent for 7-9 s. The results can be observed in Fig.24, Fig.25.

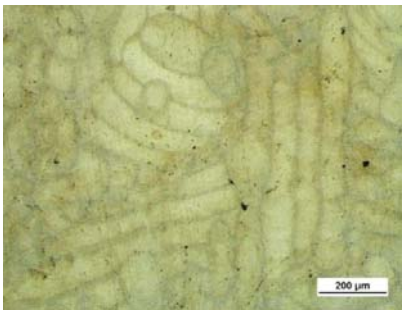

Fig. 22. 20-63 µm sample

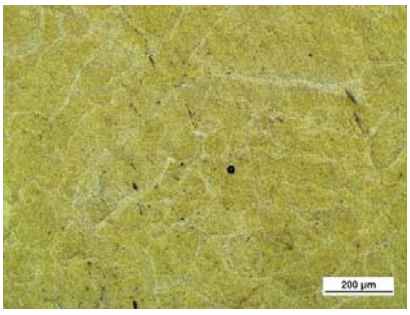

Fig. 23. 63-105 µm sample

In the depicted results could be observed the shape of the melting pools, as well as the presence of porosity. No high-density inclusions can be identified in either sample. The shape and dimension of the pattern are inhomogeneous, and no evident differences are visible between the two samples. Visually, the depth and width of the melting pools are in the same range. A thorough review of the microstructure of a typical AlSi10Mg alloy manufactured by AM can be found in [9], whose material was very similar to the one under investigation, including the size of the melting pools. The pictures give some information about the defect shape, showing the same trend in both processes: the largest defects are somehow elongated, which is a confirmation of the lack of fusion [7]. Should be noted that, as a general definition of defect size in presence of large defect densities give the possibility of cluster effect which could become a critical issue [8]. Finally, no high-density inclusions were detected in the samples.

7. Conclusion

This study has summarized the results related to a density influence analysis on AlSi10Mg produced by SLM, considering the variation of scan speed (v), point distance (Pd) and hatch spacing (Hd) while keeping the other process parameters constant. The significant results of the analysis are:

- From the optical investigation, it was revealed the fact that the higher particle size (63-105µm) had a significant influence on the density, one sample peaking at 99.9%

- The tensile test concluded with the higher particle size (63-105µm) influencing also the strength of the material, reaching a value of HV=112.16
- There was not detected the presence of high-density inclusions in the investigated samples which could affect the density and functional properties;
- Further research directions: vertical orientation investigation; microstructural changes after thermal treatment; Computed Tomography (CT) in order to determine the prospective population of defects since the manufacturing process usually causes two main defect types: gas porosity and lack of fusion [11].

8. Bibliography

[1] S.A. Jawade, Rashmi.S. Joshi, S.B.Desai (2020), Comparative study of mechanical properties of additively manufactured aluminum alloy, School of Mechanical Engineering, MIT World Peace University, materialstoday: Proceedings;
[2] Tuan D. Ngo, Alireza Kashani, Gabriele Imbalzano, Kate T.Q. Nguyen, David Hui (2018), Additive manufacturing (3D printing): A review of materials, methods, applications and challenges, Composites Part B: Engineering, Volume 143, Pages 172-196;
[3] Riccardo Casati (2019), Additive Manufacturing, Department of Mechanical Engineering, Politecnico di Milano, available on the student platform https://beep.metid.polimi.it/;
[4] K. Kempen, L. Thijsb, J. Van Humbeeckb, J.P. Krutha, Mechanical properties of AlSi10Mg produced by Selective Laser Melting, Physics Procedia 39 (2012) 439 – 446;
[5] H. Meier, Ch. Haberland (2008), Experimental studies on selective laser melting of metallic parts, Materialwissenschaft und Werkstofftechnik, Volume 39, Issue 9;
[6] R. Casati, J. Lemke, M. Vedani (2016), Microstructure and Fracture Behavior of 316L Austenitic Stainless Steel Produced by Selective Laser Melting, Journal of Materials Science & Technology, Volume 32, Issue 8, Pages 738-744;
[7] S. Romanoa, A. Brandãob, J. Gumpingerb, M. Gschweitlc, S. Berettaa (2017), Qualification of AM parts: Extreme value statistics applied to tomographic measurements, Materials & Design, volume 131, pages 32-48;
[8] Simone Romano, Angelika Brueckner-Folt, Ana Daniela Brandao, Stefano Beretta (2018), Fatigue properties of AlSi10Mg obtained by AM, Defect-based modelling and prediction of fatigue strength, Engineering Fracture Mechanics, Volume 187, Pages 165-189;
[9] Lore Thijs, Karolien Kempen, Jean-Pierre Kruth, Jan Van Humbeeck (2013), Fine-structured aluminium products with controllable textureby selective laser melting of pre-alloyed AlSi10Mg powder, Acta Materialia, Volume 61, Pages 1809-1819;
[10] Bochuan Liu, Ricky Wildman, Christopher Tuck, Ian Ashcroft, Richard Hague (2011), Investigation the effect of particle size distribution on processing parameters optimisation in selective laser melting process, Additive Manufacturing Research Group, Loughborough University;
[11] John J. Lewandowski and Mohsen Seifi (2016), Metal Additive Manufacturing A Review of Mechanical Properties, Department of Materials Science and Engineering, Case Western Reserve University (CWRU), Annu. Rev. Mater. Res. 2016. 46:151–86.

9. Notations

CAD = computer aided design
.stl = stereolitography
AM = additive manufacturing
DMD = direct metal deposition
VED = volumetric energy density
PBF = powder bed fusion
SLM = Selective Laser Melting
EBM = electron beam melting
Eρ = laser energy density
P = laser power [W]
δ = laser beam diameter [mm]
µ = laser scanning speed [mm/s]
Hd = hatch distance
Pd = point distance
v = scan speed
MP = manual polisher
SEM = scanning electron microscope
HV = Vickers hardness
CT = computed tomography